

#### Contents lists available at ScienceDirect

# Carbon

journal homepage: www.elsevier.com



# 3D bioprinted graphene oxide-incorporated matrix for promoting chondrogenic differentiation of human bone marrow mesenchymal stem cells

Xuan Zhou<sup>a</sup>, Margaret Nowicki<sup>a</sup>, Haitao Cui<sup>a</sup>, Wei Zhu<sup>a</sup>, Xiuqi Fang<sup>a</sup>, Shida Miao<sup>a</sup>, Se-Jun Lee<sup>a</sup>, Michael Keidar<sup>a, b</sup>, Lijie Grace Zhang<sup>a, b, c,</sup>

- <sup>a</sup> Department of Mechanical and Aerospace Engineering, The George Washington University, Washington DC 20052, USA
- b Department of Biomedical Engineering, The George Washington University, Washington DC 20052, USA
- <sup>c</sup> Department of Medicine, The George Washington University, Washington DC 20052, USA

#### ARTICLE INFO

#### ABSTRACT

Article history:
Received 8 December 2016
Received in revised form 15 February 2017
Accepted 16 February 2017
Available online xxx

Articular cartilage repair and regeneration are a challenging problem worldwide due to the extremely weak inherent regenerative capacity of cartilaginous tissue. As an emerging tissue engineering scaffold fabrication technology, 3D bioprinting has shown great promise in fabricating customizable artificial tissue matrices with hierarchical structures. The goal of the present study is to investigate 3D bioprinted graphene oxide (GO)-doped gelatin-based scaffolds for promoting chondrogenic differentiation of human bone marrow mesenchymal stem cells (MSCs). In the current study, GO-gelatin methacrylate (GelMA)—poly (ethylene glycol) diacrylate (PEGDA) was prepared as a biocompatible photopolymerizable bioink. GO, a multifunctional carbon based nanomaterial, was incorporated into the bioink for promoting chondrogenic differentiation. Finally, the 3D printed GelMA-PEGDA-GO scaffold with hierarchical structures was fabricated via our novel table-top stereolithography-based printer. Results showed that GelMA-PEGDA-GO scaffolds greatly promoted the glycosaminoglycan, and collagen levels after GO induced chondrogenic differentiation of hMSCs. Moreover, the Collagen II, SOX 9, and Aggrecan gene expressions associated with chondrogenesis were greatly promoted on the scaffolds. This study demonstrated that customizable 3D printed GelMA-PEGDA-GO scaffolds are excellent candidates for promoting chondrogenic differentiation of hMSCs and are therefore promising candidates for future cartilage regenerative medicine applications.

© 2016 Published by Elsevier Ltd.

#### 1. Introduction

Cartilage defects and chondral lesions resulting from trauma, osteoarthritis or disease are common and serious clinical problems in older people and athletes. For example, an estimated 46 million Americans suffer unanticipated pain, weakness, and even disability as a result of osteoarthritis alone according to the 2010 report from the National Public Health Agenda for Osteoarthritis [1]. Moreover, there are about 0.7 million hospitalizations and more than 0.6 million total joint replacements every year in the United States alone [1,2]. Approximately 22.6 billion dollars has been spent on job-related hospital costs in one year and this figure will be further expanded in the future [2]. Currently, the gold standard surgical procedures for repairing and rebuilding cartilage defects are autologous cartilage transplantation or autologous chondrocyte implantation [3]. However, these approaches are still not perfect due to limited resources of autologous cartilage tissue and cells [4]. Furthermore, articular cartilage repair and regeneration are a challenging problem worldwide due to the extremely weak inherent regenerative capacity, complex hierarchical architecture, and intricate composition of cartilaginous tissue [5]. Precious chondrocytes embedded in a dense extracellular matrix (ECM) are re-

Email address: lgzhang@gwu.edu (L.G. Zhang)

stricted from renewing and migrating largely by the lack of nutrition resupply which may restrain tissue self-repair [6].

Chondrocytes, the only cell type in articular cartilage, play a crucial role in producing and maintaining cartilaginous matrix [7]. As such, it is a commonly used cell source for articular cartilage repair and regeneration. Unfortunately, its ability to thrive is limited by a lack of resources and weak differentiation capacity, especially in seniors [8,9]. Due to the aforementioned limitation, some alternative cell sources, with improved accessibility and chondrogenic capacity, have been investigated in recent decades, such as human embryonic stem cells [10], mesenchymal stem cells (MSCs) [11], and human dermal fibroblasts [12]. In particular, human bone marrow derived MSCs are capable of differentiating into a variety of musculoskeletal cell types, such as cartilage, bone, muscle, and nerve cells; therefore they are great candidates for cartilage tissue repair [11]. Regulating culture conditions and controlling substrate properties with engineering technologies can induce hMSC differentiation into specific tissues for diverse regenerative applications.

Tissue engineering has emerged as a potential means to combine sophisticated, biomimetic scaffolds and cells for articular cartilage repair and regeneration. Various biocompatible and biodegradable scaffolds have been investigated to support structural loads, matrix deposition, and cell growth [5]. Some examples include natural [8,13] and synthetic [14,15] scaffolds, as well as those that are nanostructured [3,16] or modified with bioactive molecules [17,18]. These tissue en-

Corresponding author. 800 22nd Street NW Science and Engineering Hall, Room 3590, Washington DC 20052, USA.

gineering technologies provide a vast application prospect for cartilage repair and regeneration. The emergence of 3D bioprinting techniques has shown great promise in fabricating complex, customizable, artificial tissue matrices with hierarchical structures using computer-aided design (CAD) [19]. Stereolithography (SL), based 3D bioprinting, is an especially versatile and prevailing 3D printing technology. It uses the rapid prototyping lithographic method to photocrosslink a photocurable polymer ink, in a layer-by-layer manner, fabricating a dedicated 3D structure [19]. When compared with many other commonly used 3D bioprinting techniques, stereolithography has a high resolution capacity. Moreover, various bioactive molecules or multifunctional nanocomponents can also be directly incorporated into photocurable inks and simultaneously develop the scaffolds bioactivity and function for diverse biomedical applications [19,20]. In this study, a custom designed table top SL printer was used to fabricate a unique cartilage construct.

A novel cartilage printing ink including gelatin methacrylate (GelMA), polyethylene (glycol) diacrylate (PEGDA) and nano graphene oxide (GO) was prepared. Specially, GelMA, a major component of ECM derived from the hydrolysis of collagen, has many arginine-glycine-aspartic acids (RGD) and matrix metalloproteinase (MMP) sequences that can significantly promote cell attachment and proliferation [21,22]. Moreover, it is a photocurable biomaterial which can form matrix by photocrosslinking under UV light [22,23]. However, GelMA is often insufficient in configurability due to its weak printability performance. Herein, another widely used SL printing biomaterial, PEGDA, was blended into the GelMA bioink for improving the printability and feature resolution in this study. For the purpose of enhancing biochemical function of a GelMA-PEGDA printing ink, GO was introduced into the solution. GO is a multifunctional, bioactive nanoparticle with many unique physiochemical properties, such as carbon domains and hydrophilic functional groups, that has gained much attention for biomedical applications [24–27]. Many studies have explored the effects of graphene and GO on stem cell adhesion, growth, and differentiation [28–32]. Employing the strong adsorption capacity by  $\pi$ - $\pi$  stacking and electrostatic interaction [24], GO can induce a stem cell to differentiate into neurogenic [29], chondrogenic [30], myogenic [31], and osteogenic [32] types.

The scope of the present study is to investigate 3D bioprinted graphene oxide (GO)-doped, gelatin-based scaffolds for promoting chondrogenic differentiation of hMSCs. For this purpose, 3D printed GelMA-PEGDA-GO scaffolds with hierarchical structures were fabricated using our custom designed SL-based printer. The relevant physiochemical and biological characteristics of 3D scaffolds were examined. Moreover, type II collagen levels, glycosaminoglycan (GAG) secretion, and marker gene expression were characterized to evaluate chondrogenic differentiation of MSCs on 3D scaffolds by ELISA methods and real-time quantitative reverse transcription polymerase chain reaction (RT-PCR) assay.

# 2. Materials and methods

### 2.1. Preparation of photocrosslinkable ink

GelMA was synthesized as described in our previous work [20]. Briefly, gelatin (Type A, Sigma-Aldrich) was dissolved at 10% (w/v) into phosphate buffered saline (PBS) at 60 °C for 30 min. 4% (v/v) methacrylic anhydride was added drop-wise into gelatin solution at 50 °C for another 2 h. In order to remove excess methacrylic acid, the mixture was dialyzed in distilled water using 8–14 kDa cutoff dialy-

sis bags at 40 °C for 3 days. Lastly, the GelMA flock was obtained after lyophilization.

For GelMA-PEGDA ink preparation, PEGDA (Mn 700, Sigma-Aldrich) was mixed at 20% into 15% GelMA PBS solution containing 0.5% (w/v) 2- hydroxy-4'-(2-hydroxyethoxy)-2-methyl-propiophenone (Irgacure 2959, Sigma-Aldrich) as a photoinitiator. For GelMA-PEGDA-GO bioink preparation, different amounts of GO (Cheaptube, USA) (0, 0.05, 0.1, 0.25, 0.5 and 1 mg/mL) were fully mixed into GelMA-PEGDA bioink solution to evaluate the effect of concentration on scaffold performance.

#### 2.2. 3D printing cartilage scaffolds

The 3D printed cartilage scaffolds were fabricated using our table-top SL based printer, which consists of an X-Y axis controlled UV laser, a Z axis controlled movable stage and an interface software package (Printrum) [19,20]. The GelMA-PEGDA solutions, with or without GO bioink, were placed on the z-control movable platform and then printed by UV laser according to programmed computer aided design (CAD) models. The 3D printed GelMA-PEGDA-GO scaffolds were fabricated via a layer-by-layer process. In this work, the basic geometry pattern (wood-pile) was chosen for support scaffold. This selection is also on the base of our previously work in which we found MSCs have a higher proliferation due to its relative smaller porosity in comparison with the other pattern with same infill ratio [19]. The printing parameters are as follows: 200 µm diameter laser beam, 25 µJ intensity output of 20 kHz emitted UV, and 10 mm/s printing speed.

### 2.3. Characterization of GO and 3D printed scaffolds

UV-Vis spectra of GO was collected at a range of 200-600 nm with a Multiskan<sup>TM</sup> microplate spectrophotometer (Thermal Scientific). Fourier transform infrared (FTIR) and Raman spectra of GO were conducted within the 4000-400 cm<sup>-1</sup> wavenumber range using a Nicolet<sup>TM</sup> iS<sup>TM</sup> 50 FT-IR Spectrometer (Thermal Scientific) at room temperature. The morphologies of GO were observed by transmission electron microscopy (TEM) (FEI F200X) and atomic force microscopy (AFM) (Asylum, MFP-3D). The morphology of the 3D printed scaffolds was observed by optical microscopy (Mu800, Amscope) and further characterized by scanning electron microscope (SEM). Samples were sputter-coated with a 10 nm gold layer prior to SEM imaging. In order to investigate the mechanical properties of varied hydrogel combinations, samples were crosslinked by UV-exposure and cut into 8 mm diameter 5 mm thick, disks. The compressive modulus was determined via unconfined compression testing on a mechanical testing machine at a crosshead speed of 8 mm/min.

#### 2.4. MSC culture

Primary human bone marrow MSCs were obtained from healthy consenting donors, distributed and thoroughly characterized by the Texas A&M Health Science Center, Institute for Regenerative Medicine. Cells at passage 3–6 were used in the subsequent experiment. MSCs were cultured in Alpha Minimum Essential Medium Eagle ( $\alpha$ -MEM) supplemented with fetal bovine serum (FBS) (16.5%, v/v), penicillin/streptomycin (p/s, 1%, v/v) and L-glutamine (1%, v/v). For chondrogenic differentiation studies of MSCs, cells were cultured in  $\alpha$ -MEM supplemented with FBS (10%, v/v), penicillin and streptomycin (1%, v/v), L-glutamine (1%, v/v), dexamethasone (100 nmol/L), L-ascorbate acid (50 µg/mL), proline (40 µg/mL), sodium pyru-

vate (100 μg/mL), ITS+ (1%, v/v), and TGF-β1 (10 ng/mL) [33]. All cells were incubated at 37 °C, 5% CO<sub>2</sub> and 95% relative humidity.

#### 2.5. MSC proliferation on 3D scaffold

In order to determine optimal combinations, MSC proliferation on the scaffolds with various compositions was investigated for 5 days. These groups are PEGDA (20%), GelMA (10%), GelMA (15%), GelMA (10%) + PEGDA (20%), GelMA (15%) + PEGDA (20%), and GelMA (15%) + PEGDA (20%)+ GO (0.05, 0.1, 0.25, 0.5 and 1 mg/mL). These scaffolds were placed in a 48-well plate, and soaked in culture medium for 12 h. After pre-wetting, cells, at a density of  $5 \times 10^4$  cells/well, were seeded on the scaffolds and cultured for 1, 3 and 5 days. At the predetermined time points, the culture medium was replaced with fresh medium containing 10% CCK-8 solution (Dojindo, Japan) and incubated for 2 h. Lastly, 100 μL of culture medium was transferred into a new 96-well plate and the absorbance was recorded by Spectrophotometer (Thermo, USA) at a wavelength of 450 nm. After day 5, MSC morphology was imaged by a laser confocal microscope (Carl Zeiss LSM 710). All scaffolds were rinsed with PBS and processed with 10% formalin and 0.1% Triton-100 respectively for 10 min each. Lastly, the cells on the scaffolds were stained with Texas Red-X phalloidin for 30 min followed by 4', 6-diamidino-2-phenylindole (DAPI) for another 15 min.

#### 2.6. Protein adsorption capacity of 3D printed GO scaffold

Bovine Serum Albumin (BSA) as a model protein was employed for investigating the protein reconcentration capacity of the scaffold with GO. Briefly, the scaffolds were soaked in 40 μg/mL BSA PBS solution at 37 °C for 24 h. After incubation, the scaffolds were taken out and the concentration of BSA was quantified by BCA<sup>TM</sup> protein assay (Thermo, USA). The absorbance was recorded spectrophotometrically at 562 nm according to the manufacturer's instructions.

#### 2.7. Chondrogenic differentiation of MSCs on scaffolds

MSCs were induced toward chondrogenic differentiation for evaluating cartilage potential on each scaffold. MSCs were seeded at a density of  $2\times10^5$  cells/well on each scaffold, in a proliferation medium, and incubated for 24 h. Subsequently, the medium was replaced with fresh differentiation medium and continuously cultured for 3 weeks. At predetermined time intervals, the scaffolds were rinsed with PBS and then used for histochemical examination and biochemical analysis.

Histochemical staining of chondrogenesis was examined by Alcian Blue assay [34]. Briefly, scaffolds were fixed with 10% formalin for 30 min and rinsed. The differentiated cells on each scaffold were stained with 1% Alcian Blue solution (in 3% acetic acid, pH 2.5) (8GX, Sigma) for 20 min. After staining, excess stain was removed and scaffolds were fully rinsed and imaged using a microscope.

Collagen II secretion, glycosaminoglycan (GAG) synthesis, and total collagen levels were analyzed for evaluating chondrogenic performance. The specimens were enzymatically digested in a Papain-based solution at 60 °C for 18 h. The aliquots were then taken out for chondrogenic biochemical analysis. Collagen II was examined via a type II collagen ELISA kit (TSZ ELISA, USA) per the manufacturer's instructions. Briefly, aliquots were added to a pre-coated 96-well plate and incubated at 60 °C for 18 h. Unbound sample was rinsed, Biotinylated Antibody was added to each well, and the plate was incubated for 20 min. After removing the antibody and washing the plate, the enzyme was added before again incubating the plate and

rinsing. Lastly, a stop solution was mixed with the enzyme and the absorbance was recorded at 450 nm.

GAG content was quantified by 1, 9-dimethylmethylene blue (DMB, Sigma) assay. DMB solution was prepared by dissolving 16 mg DMB, 3.04 g glycine, 1.6 g NaCl, and 95 mL of 0.1 M acetic acid into 1 L pure water, followed by 0.45  $\mu$ m filtering and protecting from light. 200  $\mu$ L of DMB solution was mixed into 50  $\mu$ L digested aliquots in a 96-well plate and gently shaken for 10 s. The absorbance was then recorded at 524 nm.

Total collagen level was determined by Sirius red colorimetric assay.  $100~\mu L$  digested aliquots were added into a 96-well plate and dried overnight. The specimens were fully rinsed with pure water.  $150~\mu L$  of 0.1% Picro-sirius red solution (w/v, Direct Red 80 in Picric acid, Sigma) was added into each well for 1 h incubation at room temperature. Each well was fully rinsed with 5% acidified water (v/v, Glacial acetic acid in Distilled water) and followed by additional  $150~\mu L$  of 0.1~M NaOH solution for 30 min incubation at room temperature. The supernatants in each well were transferred into a new 96-well plate and recorded at 550~nm.

#### 2.8. Real Time PCR analysis

The Collagen II, SOX 9, Aggrecan marker gene expressions related with chondrogenesis were investigated by a Real Time-PCR assay [35]. After 1, 2 and 3 weeks of chondrogenic differentiation, the specimens were fully rinsed with PBS and then treated with 1 mL TRIzol Reagent (Thermolfisher, USA) for 30 min. Total RNA was extracted using a standard TRIzol protocol. The cDNA was synthesized using a Real-time PT-PCR kit (PrimeScript RT Master Mix, Takara) according to the manufacturer's instructions. Quantitative PCR analysis was performed in triplicate per sample using SYBR qPCR kit (SYBR Premix Ex Taq II(Tli RNase H Plus), Takara) and CFX384 Real-Time System (Bio-Rad, USA). Relative quantification of gene expression was analyzed using standard 2<sup>-(ΔΔCt)</sup> method and glyceraldehyde 3-phosphate dehydrogenase (GAPDH) was used as the endogenous housekeeping gene. The detailed PCR primer sequences are available in Table S1.

#### 2.9. Statistical analysis

Data are presented as mean  $\pm$  standard deviation and analyzed by one-way ANOVA methods. A p < 0.05 was considered statistically significant to evaluate the significance of the experimental data.

#### 3. Results and discussion

#### 3.1. 3D printed scaffold fabrication and characterization

Fig. 1 summarizes the fabrication of the novel 3D printed scaffolds for promoting chondrogenic differentiation of MSCs. Pre-designed CAD models and surface plots of the 3D printed scaffolds are shown in Fig. 2(A and B) and Fig. 2(C and D), respectively. SEM was used to characterize the morphology of the 3D scaffolds, without or with GO (Fig. 2(E and F)). A smooth surface, coupled with uniform pores and orderly channels, was observed clearly in scaffolds, which closely matched the pre-designed CAD models. Furthermore, it was found that the GO incorporation did not influence the structural fabrication. The scaffold with hierarchical structure was successfully prepared via our novel stereolithography based 3D printer.

UV–vis spectroscopy, Raman and FTIR spectra of GO were characterized and the results are shown in Fig. 3. An absorption peak at 230 nm was found in spectra which is ascribed to the  $\pi$ - $\pi$ \* transition

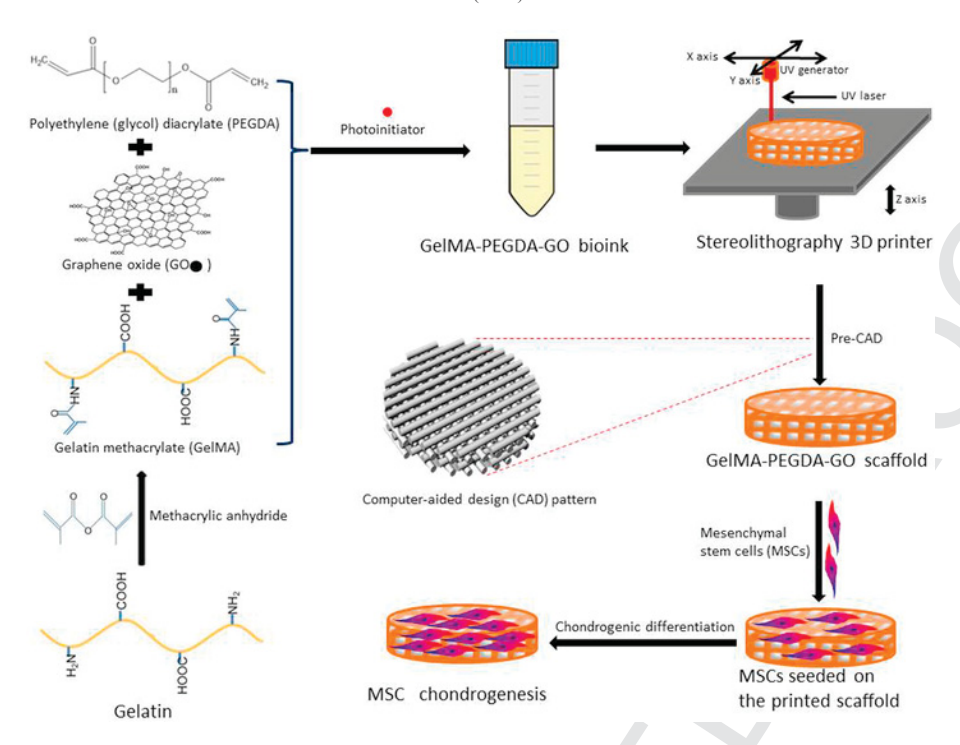


Fig. 1. Schematic diagram of 3D printed GO scaffold for promoting chondrogenic differentiation of hMSCs.

of aromatic C—C bonds (Fig. 3A) [24,36]. The Raman spectrum is presented in Fig. 3B. Two prominent peaks located at 1355 and 1605 cm<sup>-1</sup> were noted and can be attributed to the G band and D band in GO, respectively. The G band and D band are related to the E2g phonon of sp2 atoms and breathing mode of sp2 rings, respectively [24,36]. The FTIR spectrum is shown as Fig. 3C. There are some oxygen functional groups noted in the spectra as well. The broad and wide peak at 3215 cm-1 can be attributed to the hydroxyl group (O—H) stretching vibrations of the C—OH groups in GO and H—OH in the environment. The sharp peak at 1718 and 1618 cm<sup>-1</sup> are assigned to the carbonyl/carboxy (C=O) and aromatics (C=C) bands respectively. The absorption band at 1050 cm<sup>-1</sup> can be ascribed to alkoxy (C -O) stretching vibration [24,36]. The morphology of GO was characterized by TEM (Fig. 3D) and AFM (Fig. 3(E and F)). The GO size presents the width of 3-5 µm and the height of 0.75 nm which correspond to two graphene oxide layers.

In order to investigate the mechanical property of the inks, different GelMA-PEGDA combinations and GO concentration incorporations were evaluated. The corresponding compressive modulus is represented in Figs. S1A and S1B, respectively. The results show that the compressive modulus increased with GelMA concentration and was greatly enhanced by PEGDA incorporation. Additionally, the GO incorporation did not influence the compressive modulus of the scaffold with the exception of the max GO concentration of 1 mg/mL. This result can be explained that the relatively low GO mass ratio incorporated in ink even in max concentration. The influence on the compressive modulus of the scaffold was insignificant.

## 3.2. Proliferation of MSCs on 3D scaffold

MSC proliferation on various 3D printed scaffolds, with different compositions, was investigated for 5 days (Fig. 4). Fig. 4A shows MSC proliferation with various ratios of GelMA and PEGDA. MSCs grew well on the GelMA and GelMA-PEGDA hydrogels when compared to the PEGDA hydrogel on Day 5. The MSC proliferation on

10% and 15% GelMA groups is higher than the corresponding 10% and 15% GelMA+ 20% PEGDA groups, respectively. Moreover, the MSC proliferation on hydrogels containing 15% GelMA is higher than that of 10% GelMA. Considering the printability of inks, and balancing compatibility and mechanical performance, 15% GelMA+ 20% PEGDA will be chosen as the optimal ink composition, despite a slight decrease in MSC proliferation resulting from the PEGDA blending when compared to GelMA only samples.

MSC proliferation on 15% GelMA+ 20% PEGDA (hereinafter referred to as 15% GelMA + PEGDA) incorporated with different concentrations of GO are shown in Fig. 4B. MSCs grew faster on all groups with time and the highest proliferation was found in 0.1 mg/ mL incorporation group on day 5, an increase of 22% when compared to that without GO incorporation. This phenomenon was confirmed by confocal microscopy images, Fig. 5. MSCs spread and extended excellently on scaffolds with incorporated GO (0-0.25 mg/mL) after 5 days of culture. The cytoskeleton and cell nuclei were clearly observed on the scaffolds. MSCs are long and thin, and the actin fibers fully spread on the scaffold. This fibroblast-like morphology is typical feature of MSC. Appropriate GO incorporation can promote MSC adhesion, growth, and differentiation. This is in agreement with literature and it may be related to the strong adsorption capacity of GO by  $\pi$ - $\pi$  stacking and electrostatic interaction [28,30,32]. It is can be considered that this adsorptive performance will be favorable to FBS adsorption and subsequent cell proliferation on scaffold. There is more discussion on this topic in the next section. Ultimately, the 15% GelMA + PEGDA with GO incorporated at 0.1 mg/mL was screened as an optimal combination for subsequent MSC differentiation study.

#### 3.3. Protein reconcentrated capacity of GelMA-PEGDA-GO scaffold

Surface characteristics, such as protein affinity, of the scaffold are crucial features for regulating or influencing cell behaviors such as adhesion, proliferation, differentiation, and morphology [37,38].

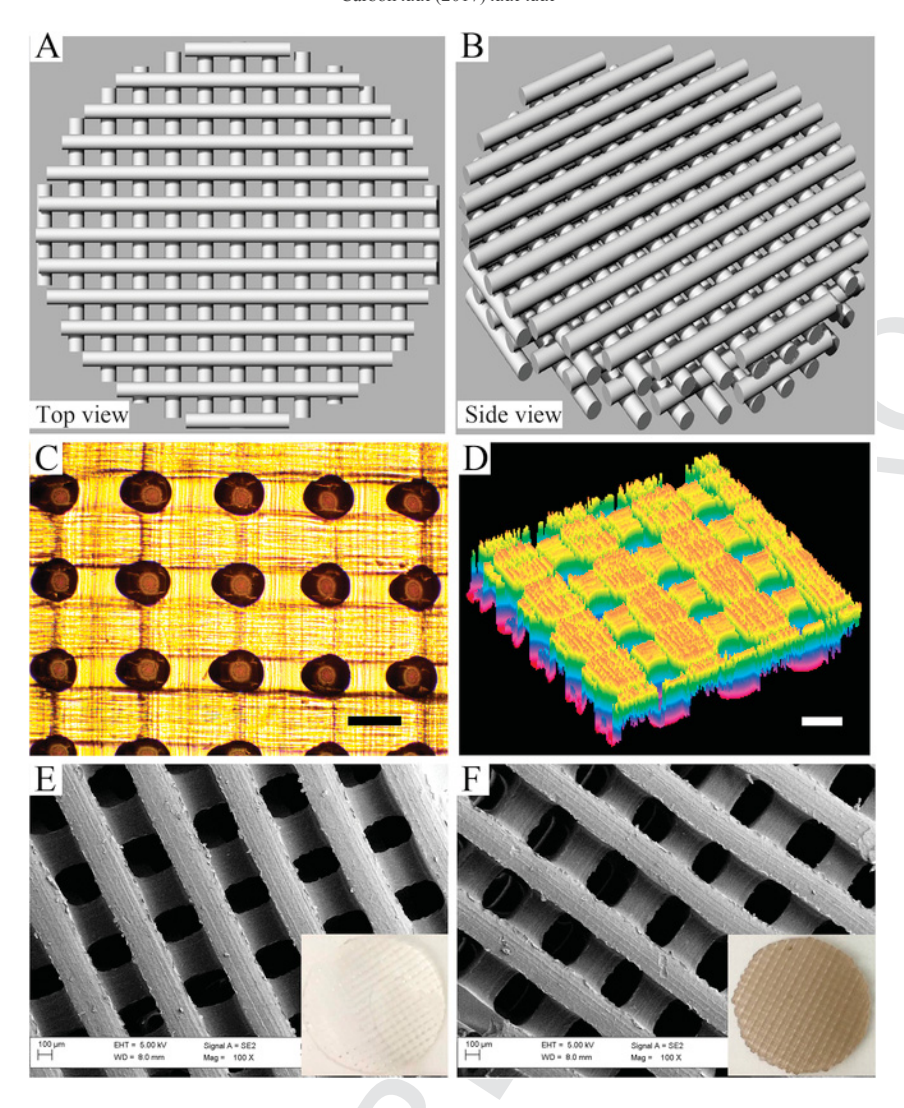


Fig. 2. (A–B) Top and side views of the CAD 3D scaffold model. (C) Microscope image and (D) surface plot of GelMA-PEGDA scaffold without GO; Scale bar = 200 μm. (E–F) SEM micrographs of GelMA-PEGDA scaffold without GO and with GO (0.1 mg/mL). The inset images are photographs of the corresponding scaffolds. (A colour version of this figure can be viewed online.)

BSA, as a model protein, was employed to evaluate the protein affinity of GelMA-PEGDA scaffolds incorporated with and without GO (Fig. 6). The adsorption profiles show that BSA levels on GelMA-PEGDA-GO scaffolds were 763% higher than that of GelMA-PEGDA scaffolds after 24 h; the protein adsorption capacity on both of the scaffolds became saturated after 24 h. The results indicated that GO-incorporated scaffolds were able to adsorb significantly more protein than those without GO. From this it was implied that GO could effectively improve the protein affinity of substrates. Some researchers have reported that GO has extraordinary adsorption capacity for proteins [39], DNA [40], and small molecule drugs [41] via  $\pi$ - $\pi$  stacking and electrostatic interaction [24]. This behavior promotes deposition of nutritious components (for instance: FBS) on the scaffold surface and is favorable for cell proliferation and survival. It was expected that this deposition will promote MSC behaviors of adhesion and growth on scaffolds. This performance is highly connected with the proliferation results of MSCs on the 3D scaffolds mentioned above.

# 3.4. Chondrogenic differentiation of MSCs on GelMA-PEGDA-GO scaffold

Under specified culture conditions, MSCs can be induced into chondrogenesis and form cartilage for tissue regeneration. A three week chondrogenic differentiation study was conducted on the GelMA-PEGDA-GO scaffolds. The results of the qualitative histochemical staining and biochemical quantitative analysis including collagen II, GAG, and total collagen synthesis, at predetermined time points, are shown in Figs. 7 and 8.

Alcian Blue is a common and reliable heteroglycan stain for GAG in cartilage and other extracellular matrices. It was found that the extracellular product was stained and exhibited bluish-green or blue after 3 weeks when compared to that of the bare scaffold (Fig. 7). In this experiment, the MSCs were induced into chondrogenic differentiation. In this status, the MSCs did not have multipotent anymore and tended to synthesize specific chondrogenic extracellular matrices. The cells are round-like shape and can be stained by Alcian Blue solution. Moreover, the color on the GelMA-PEGDA-GO scaffold was slightly darker than that of the GelMA-PEGDA scaffold. It implied

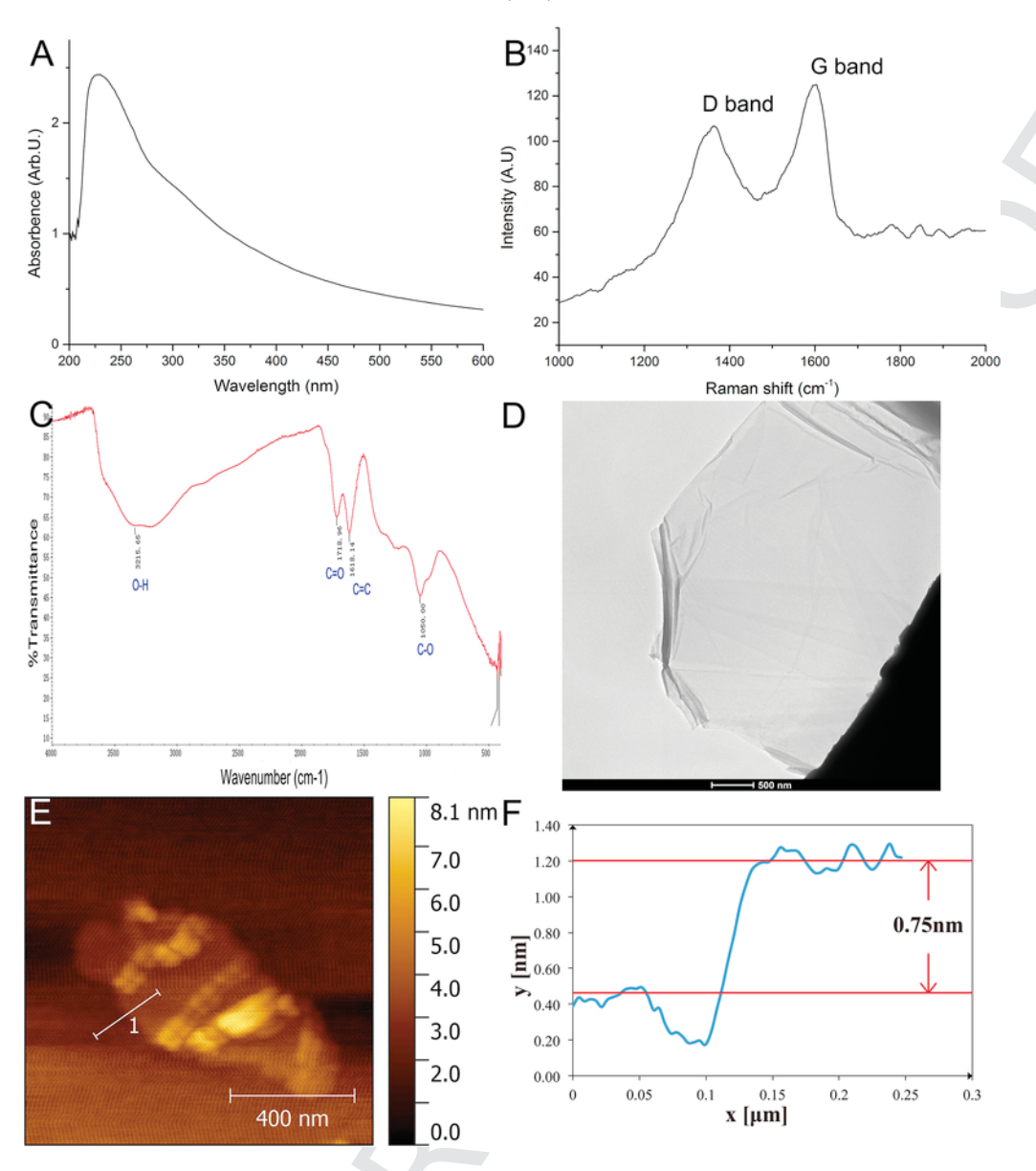


Fig. 3. (A) UV-vis spectroscopy, (B) Raman, (C) FTIR spectra, (D) TEM, (E) AFM images, and (F) the height diagram of GO sample. (A colour version of this figure can be viewed online.)

that more GAG was synthesized on the former scaffold than the later after chondrogenic differentiation. Furthermore, the results were verified by quantitative biochemical analysis of collagen II, GAG, and total collagen (Fig. 8). After 3 weeks, the collagen II synthesis, GAG secretion, and total collagen level on the GelMA-PEGDA-GO scaffold were dramatically greater, by 66%, 71% and 43% respectively, than those on the GelMA-PEGDA scaffold. This data indicates that GO incorporation remarkably enhances chondrogenic differentiation. Type II collagen and GAG are essential ECM components in articular cartilage and their production directly correlates to the level of chondrogenesis. In this study, GO incorporation enhanced scaffold performance greatly, improving chondrogenic differentiation of MSCs; this enhanced performance can mainly be ascribed to the accessional biological function of GO [30,42]. This phenomenon could be explained by incorporated GO acting as a pre-concentration platform for chondrogenic inducers (such as FBS and TGF-β1) accelerating their specific differentiation into chondrogenesis [28,30]. It was considered

that GO incorporation could stably adsorb TGF-β1 which was introduced directly to MSCs and then enhance the chondrogenic differentiation of MSCs [30]. This behavior greatly promoted MSC adhesion and chondrogenesis on scaffolds.

# 3.5. Quantitative analysis of Real Time PCR on chondrogenic differentiation

For the purpose of further investigating the effect of GO on chondrogenic differentiation of MSCs on the scaffold, the tissue-specific gene expression of type II collagen, SOX-9, and aggrecan were evaluated from gene level (Fig. 9). After 3 weeks, the gene marker expression of collagen II, SOX-9, and aggrecan on the GelMA-PEGDA-GO scaffold was significantly greater than that on the GelMA-PEGDA scaffold by 83%, 44%, and 101%, respectively. These results are highly consistent with biochemical analyses mentioned above. Compared to biochemical quantitative examination,

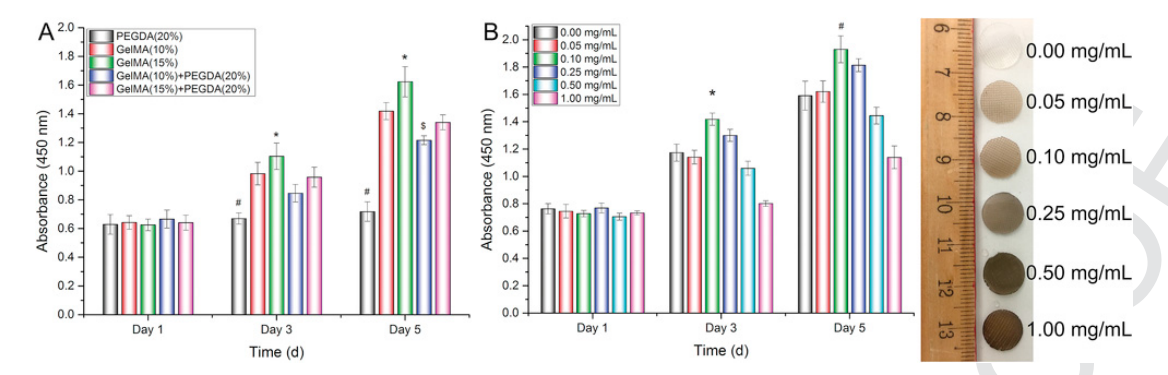
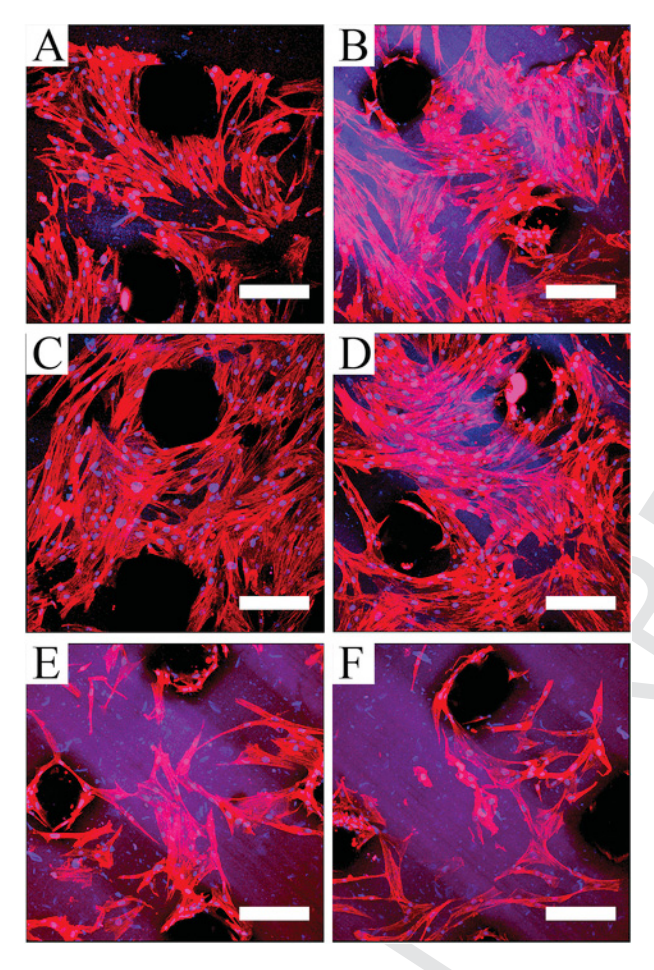
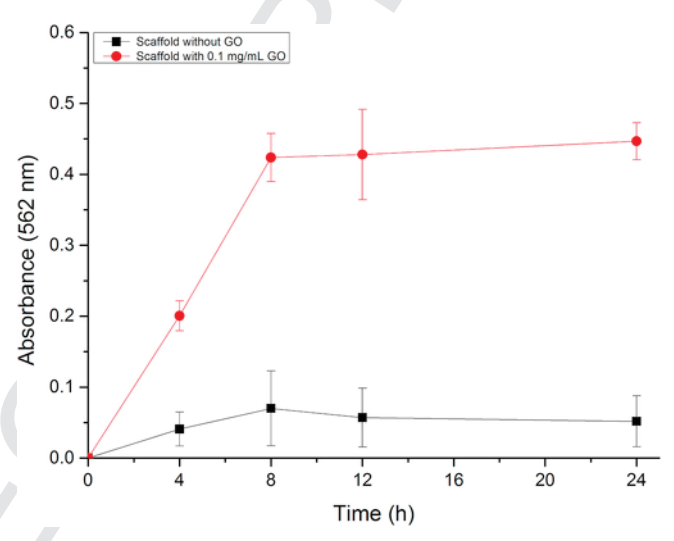


Fig. 4. (A) MSC proliferation on hydrogels with different compositions for 5 days. Data are mean  $\pm$  standard deviation, n=8. #p < 0.05 when compared to all other groups at respective time points. Day 3: \*p < 0.05 when compared to GelMA (10%)+PEGDA (20%) group. Day 5: \*p < 0.05 and \$p < 0.05 when compared to all other groups. (B) MSC proliferation on GelMA-PEGDA scaffolds incorporated with different concentrations of GO for 5 days. The photographs are the corresponding scaffolds. Data are mean  $\pm$  standard deviation, n=8. \*p < 0.05 when compared to all other groups at day 3. #p < 0.05 when compared to all other groups excepting the 0.25 mg/mL group. (A colour version of this figure can be viewed online.)



**Fig. 5.** Confocal micrographs of 5-day MSC proliferation on GelMA-PEGDA scaffolds incorporated with (A) 0 mg/mL, (B) 0.05 mg/mL, (C) 0.10 mg/mL, (D) 0.25 mg/mL, (E) 0.50 mg/mL, and (F) 1 mg/mL concentrations of GO. Scale bar = 200 μm. The cytoskeleton and cell nuclei were stained by Texas Red<sup>®</sup>-X phalloidin (red) and DAPI (Blue). (A colour version of this figure can be viewed online.)

RT-PCR is more precise and accurate when analyzing the up or down regulation of specific gene expressions in cells. Collagen II and aggrecan genes are key markers relevant to chondrocyte-specific ECM for cartilage generation. Type II collagen, a primary component in cartilage, provides structure and protection for the joint and for the



**Fig. 6.** Adsorption profiles of BSA on GelMA-PEGDA scaffolds with and without GO (0.1 mg/mL) at different time points. Data are mean  $\pm$  standard deviation, n = 8. (A colour version of this figure can be viewed online.)

end of the bone. Aggrecan genes express a type of protein relevant with proteoglycan which associates with other components (collagen, glycoprotein, fibronectin, etc.) to organize cartilage structures. These Real-Time PCR results sufficiently support more extensive expression of chondrogenic genes on the GelMA-PEGDA-GO scaffold. The SOX-9 gene is another crucial marker relevant to the transcription factor for cartilage generation [42,43]. SOX-9 involves the high-mobility-group (HMG) domain transcription factor which is mainly expressed in chondrocytes and cartilage relevant tissues, and usually coincident with the expression of type II collagen [44]. The resultant gene expression demonstrated upregulation of SOX-9 on GO-incorporated scaffolds. The Real Time PCR revealed that GelMA-PEGDA-GO 3D scaffolds showed enhanced interaction for chondrogenic signaling cascades. The phenomena also can be explained as the aforementioned "pre-concentration platform" effect. Cartilage specific gene expression of type II collagen, SOX-9, and aggrecan were up-regulated in the GO incorporated group. Comprehensively, the above differentiation results suggest that GO incorporation in scaffolds greatly enhanced tissue-specific gene expression of type II collagen, SOX-9 and aggrecan, and could prominently promote chondrogenic differentiation of MSCs into cartilage.

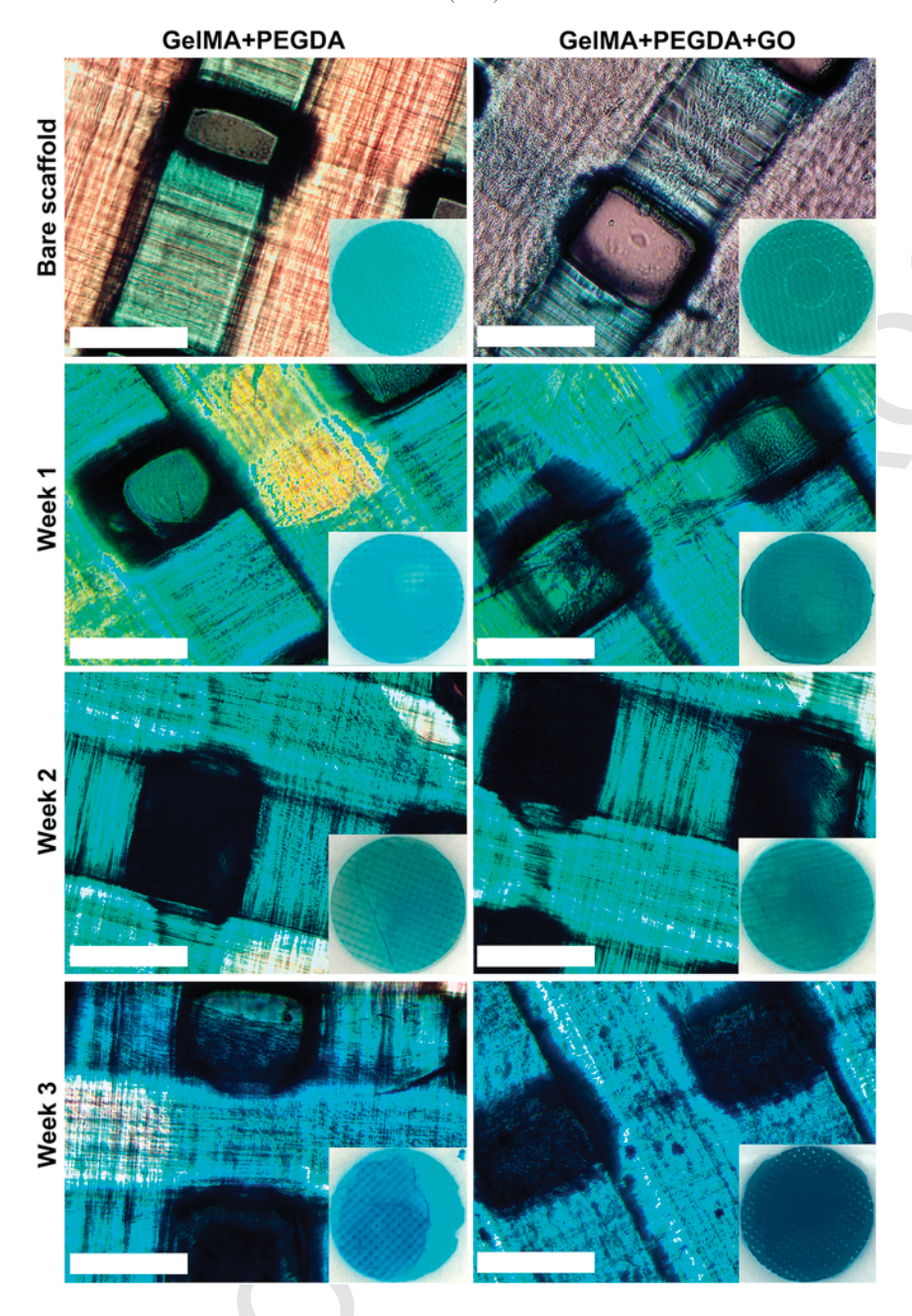


Fig. 7. Alcian Blue stained micrographs of MSCs after chondrogenic differentiation on the surface of the GelMA-PEGDA scaffolds without and with GO over 3 weeks. Scale bar =  $200 \, \mu m$ . (A colour version of this figure can be viewed online.)

## 4. Conclusions

In summary, a customizable, 3D printed, GO incorporated matrix (GelMA-PEGDA-GO) with hierarchical structure was successfully fabricated via our table-top stereolithography-based printer. The resulting scaffolds exhibited favorable mechanical properties and excellent biocompatibility. GelMA-PEGDA-GO scaffolds were able to adsorb much more protein than those without GO. This improved protein-like adsorption contributed to improving cell adhesion on the surface of the scaffold, and was also responsible for higher cell proliferation and differentiation on GelMA-PEGDA-GO scaffolds when compared to GelMA-PEGDA scaffolds. Most importantly, GelMA-PEGDA-GO scaffolds greatly promoted the glycosaminoglycan,

protein, and collagen levels after GO induced chondrogenic differentiation of hMSCs. In particular, the most significant improvement is the chondrogenic gene expression of type II Collagen, SOX-9 and aggrecan observed on the 3D GelMA-PEGDA-GO scaffolds. This study demonstrated that customizable 3D printed GelMA-PEGDA-GO scaffolds are excellent candidates for promoting chondrogenic differentiation of hMSCs showing great promise for future cartilage regeneration.

#### Acknowledgments

The authors thank the financial support from NSF BME program grant # 1510561 and the George Washington University Center for Microscopy and Image Analysis for imaging support.

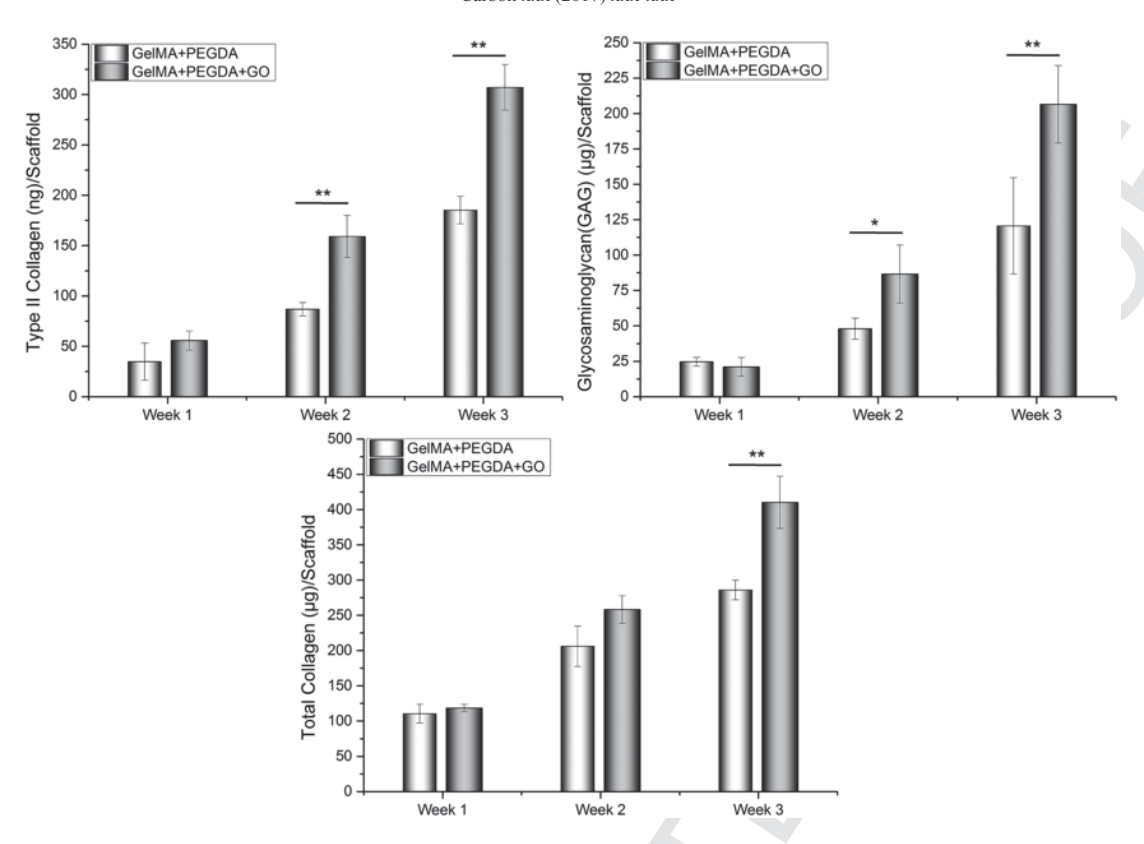


Fig. 8. (A) Collagen II, (B) GAG and (C) total collagen secretion of MSCs after chondrogenic differentiation on GelMA-PEGDA scaffolds without and with GO over 3 weeks. Data are mean  $\pm$  standard deviation, n = 8. \*p < 0.05 and \*\*p < 0.01.

# Appendix A. Supplementary data

Supplementary data related to this article can be found at http://dx. doi.org/10.1016/j.carbon.2017.02.049.

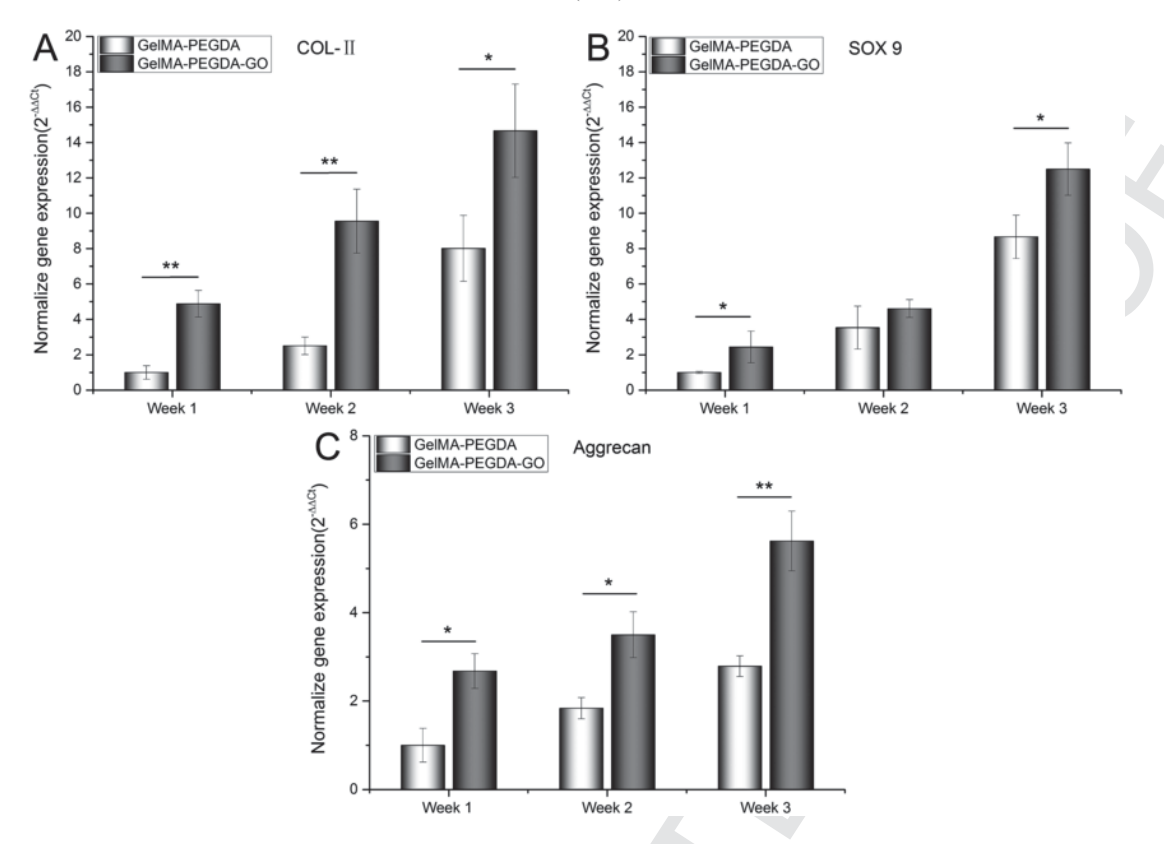


Fig. 9. Normalized gene expression (Col-II, SOX 9 and Aggrecan) of MSCs after chondrogenic differentiation on GelMA-PEGDA scaffolds without and with GO over 3 weeks. Data are mean  $\pm$  standard deviation, n = 6. \*p < 0.05 and \*\*p < 0.01.

#### References

- D. Lubar, P.H. White, L.F. Callahan, R.W. Chang, C.G. Helmick, D.R. Lappin, et al., A national public Health Agenda for osteoarthritis 2010, Semin. Arthritis Rheum. 39 (5) (2010) 323–326.
- [2] E. Yelin, S. Weinstein, T. King, The burden of musculoskeletal diseases in the United States. Semin. Arthritis Rheum. (2016)().
- [3] R.N. Shah, N.A. Shah, M.M. Del Rosario Lim, C. Hsieh, G. Nuber, S.I. Stupp, Supramolecular design of self-assembling nanofibers for cartilage regeneration, Proc. Natl. Acad. Sci. 107 (8) (2010) 3293–3298.
- [4] D.J. Huey, J.C. Hu, K.A. Athanasiou, Unlike bone, cartilage regeneration remains elusive, Science 338 (6109) (2012) 917–921.
- [5] L. Zhang, J. Hu, K.A. Athanasiou, The role of tissue engineering in articular cartilage repair and regeneration, Crit. Rev. Bioeng. 37 (1–2) (2009) 1–57.
- [6] J. Becerra, J.A. Andrades, E. Guerado, P. Zamora-Navas, J.M. López-Puertas, A.H. Reddi, Articular cartilage: structure and regeneration, Tissue Eng. Part B 16 (6) (2010) 617–627.
- [7] K. Von Der Mark, V. Gauss, H. Von Der Mark, P. Muller, Relationship between cell shape and type of collagen synthesised as chondrocytes lose their cartilage phenotype in culture, Nature 267 (5611) (1977) 531–532.
- [8] Y. Wang, D.J. Blasioli, H.-J. Kim, H.S. Kim, D.L. Kaplan, Cartilage tissue engineering with silk scaffolds and human articular chondrocytes, Biomaterials 27 (25) (2006) 4434–4442.
- [9] A. Barbero, S. Grogan, D. Schäfer, M. Heberer, P. Mainil-Varlet, I. Martin, Age related changes in human articular chondrocyte yield, proliferation and post-expansion chondrogenic capacity, Osteoarthr. Cartil. 12 (6) (2004) 476–484.
- [10] W.S. Toh, E.H. Lee, X.-M. Guo, J.K.Y. Chan, C.H. Yeow, A.B. Choo, et al., Cartilage repair using hyaluronan hydrogel-encapsulated human embryonic stem cell-derived chondrogenic cells, Biomaterials 31 (27) (2010) 6968–6980.
- [11] M.F. Pittenger, A.M. Mackay, S.C. Beck, R.K. Jaiswal, R. Douglas, J.D. Mosca, et al., Multilineage potential of adult human mesenchymal stem cells, Science 284 (5411) (1999) 143–147.
- [12] J.P.E. Junker, P. Sommar, M. Skog, H. Johnson, G. Kratz, Adipogenic, chondrogenic and osteogenic differentiation of clonally derived human dermal fibroblasts, Cells Tissues Organs 191 (2) (2010) 105–118.

- [13] W. Dai, N. Kawazoe, X. Lin, J. Dong, G. Chen, The influence of structural design of PLGA/collagen hybrid scaffolds in cartilage tissue engineering, Biomaterials 31 (8) (2010) 2141–2152.
- [14] S.C. Neves, L.S. Moreira Teixeira, L. Moroni, R.L. Reis, C.A. Van Blitterswijk, N.M. Alves, et al., Chitosan/Poly( -caprolactone) blend scaffolds for cartilage repair, Biomaterials 32 (4) (2011) 1068–1079.
- [15] J.M. Coburn, M. Gibson, S. Monagle, Z. Patterson, J.H. Elisseeff, Bioinspired nanofibers support chondrogenesis for articular cartilage repair, Proc. Natl. Acad. Sci. 109 (25) (2012) 10012–10017.
- [16] D. Puppi, F. Chiellini, A.M. Piras, E. Chiellini, Polymeric materials for bone and cartilage repair, Prog. Polym. Sci. 35 (4) (2010) 403–440.
- [17] P. Orth, G. Kaul, M. Cucchiarini, D. Zurakowski, M.D. Menger, D. Kohn, et al., Transplanted articular chondrocytes co-overexpressing IGF-I and FGF-2 stimulate cartilage repair in vivo, Knee Surg. Sports Traumatol. Arthrosc. 19 (12) (2011) 2119–2130.
- [18] H. Madry, P. Orth, G. Kaul, D. Zurakowski, M.D. Menger, D. Kohn, et al., Acceleration of articular cartilage repair by combined gene transfer of human insulin-like growth factor I and fibroblast growth factor-2 in vivo, Arch. Orthop. Trauma Surg. 130 (10) (2010) 1311–1322.
- [19] X. Zhou, N.J. Castro, W. Zhu, H. Cui, M. Aliabouzar, K. Sarkar, et al., Improved human bone marrow mesenchymal stem cell osteogenesis in 3D bioprinted tissue scaffolds with low intensity pulsed ultrasound stimulation, Sci. Rep. 6 (2016) 32876.
- [20] X. Zhou, W. Zhu, M. Nowicki, S. Miao, H. Cui, B. Holmes, et al., 3D bioprinting a cell-laden bone matrix for breast cancer metastasis study, ACS Appl. Mater. Interfaces 8 (44) (2016) 30017–30026.
- [21] J.W. Nichol, S.T. Koshy, H. Bae, C.M. Hwang, S. Yamanlar, A. Khademhosseini, Cell-laden microengineered gelatin methacrylate hydrogels, Biomaterials 31 (21) (2010) 5536–5544.
- [22] K. Yue, G. Trujillo-de Santiago, M.M. Alvarez, A. Tamayol, N. Annabi, A. Khademhosseini, Synthesis, properties, and biomedical applications of gelatin methacryloyl (GelMA) hydrogels, Biomaterials 73 (2015) 254–271.
- [23] X. Zhao, Q. Lang, L. Yildirimer, Z.Y. Lin, W. Cui, N. Annabi, et al., Photocrosslinkable gelatin hydrogel for epidermal tissue engineering, Adv. Healthc. Mater 5 (1) (2016) 108–118.
- [24] Y. Chong, Y. Ma, H. Shen, X. Tu, X. Zhou, J. Xu, et al., The in vitro and in vivo toxicity of graphene quantum dots, Biomaterials 35 (19) (2014) 5041–5048

- [25] A. Shashurin, M. Keidar, Synthesis of 2D materials in arc plasmas, J. Phys. D. Appl. Phys. 48 (31) (2015) 314007.
- [26] X. Fang, A. Shashurin, M. Keidar, Role of substrate temperature at graphene synthesis in an arc discharge, J. Appl. Phys. 118 (10) (2015) 103304.
- [27] X. Fang, A. Shashurin, G. Teel, M. Keidar, Determining synthesis region of the single wall carbon nanotubes in arc plasma volume, Carbon 107 (2016) 273–280
- [28] W.C. Lee, C.H.Y.X. Lim, H. Shi, L.A.L. Tang, Y. Wang, C.T. Lim, et al., Origin of enhanced stem cell growth and differentiation on graphene and graphene oxide, ACS Nano 5 (9) (2011) 7334–7341.
- [29] S.Y. Park, J. Park, S.H. Sim, M.G. Sung, K.S. Kim, B.H. Hong, et al., Enhanced differentiation of human neural stem cells into neurons on graphene, Adv. Mater 23 (36) (2011) H263–H267.
- [30] H.H. Yoon, S.H. Bhang, T. Kim, T. Yu, T. Hyeon, B.S. Kim, Dual roles of graphene oxide in chondrogenic differentiation of adult stem cells: cell-adhesion substrate and growth factor-delivery carrier, Adv. Funct. Mater 24 (41) (2014) 6455–6464.
- [31] S.H. Ku, C.B. Park, Myoblast differentiation on graphene oxide, Biomaterials 34 (8) (2013) 2017–2023.
- [32] T.R. Nayak, H. Andersen, V.S. Makam, C. Khaw, S. Bae, X. Xu, et al., Graphene for controlled and accelerated osteogenic differentiation of human mesenchymal stem cells, ACS Nano 5 (6) (2011) 4670–4678.
- [33] L.A. Solchaga, K.J. Penick, J.F. Welter, Chondrogenic differentiation of bone marrow-derived mesenchymal stem cells: tips and tricks, Methods Mol. Biol. 698 (2011) 253–278.
- [34] B. Delorme, P. Charbord, Culture and characterization of human bone marrow mesenchymal stem cells, Methods Mol. Med. 140 (2007) 67–81.
- [35] I. Sekiya, J.T. Vuoristo, B.L. Larson, D.J. Prockop, In vitro cartilage formation by human adult stem cells from bone marrow stroma defines the se-

- quence of cellular and molecular events during chondrogenesis, Proc. Natl. Acad. Sci. 99 (7) (2002) 4397–4402.
- [36] E.-Y. Choi, T.H. Han, J. Hong, J.E. Kim, S.H. Lee, H.W. Kim, et al., Noncovalent functionalization of graphene with end-functional polymers, J. Mater. Chem. 20 (10) (2010) 1907–1912.
- [37] K.M. Woo, J. Seo, R. Zhang, P.X. Ma, Suppression of apoptosis by enhanced protein adsorption on polymer/hydroxyapatite composite scaffolds, Biomaterials 28 (16) (2007) 2622–2630.
- [38] N.M. Alves, I. Pashkuleva, R.L. Reis, J.F. Mano, Controlling cell behavior through the design of polymer surfaces, Small 6 (20) (2010) 2208–2220.
- [39] W. Hu, C. Peng, M. Lv, X. Li, Y. Zhang, N. Chen, et al., Protein corona-mediated mitigation of cytotoxicity of graphene oxide, ACS Nano 5 (5) (2011) 3693–3700.
- [40] M. Wu, R. Kempaiah, P.-J.J. Huang, V. Maheshwari, J. Liu, Adsorption and desorption of DNA on graphene oxide studied by fluorescently labeled oligonucleotides, Langmuir 27 (6) (2011) 2731–2738.
- [41] S. Goenka, V. Sant, S. Sant, Graphene-based nanomaterials for drug delivery and tissue engineering, J. Control. Release 173 (2014) 75–88.
- [42] J. Park, I.Y. Kim, M. Patel, H.J. Moon, S.J. Hwang, B. Jeong, 2D and 3D hybrid systems for enhancement of chondrogenic differentiation of tonsil-derived mesenchymal stem cells, Adv. Funct. Mater 25 (17) (2015) 2573–2582.
- [43] W.C. Lee, C.H. Lim, C. Su, K.P. Loh, C.T. Lim, Cell-assembled graphene biocomposite for enhanced chondrogenic differentiation, Small 11 (8) (2015) 963–969
- [44] W. Bi, J.M. Deng, Z. Zhang, R.R. Behringer, B. de Crombrugghe, Sox9 is required for cartilage formation, Nat. Genet. 22 (1) (1999) 85–89.